



## Paleomagnetic study of El Metate shield volcano (Michoacán, Mexico) confirms its monogenetic nature and young age ( 1250 CE)

Ahmed Nasser Mahgoub, Harald Böhnelt, Claus Siebe, Magdalena Oryaëlle Chevrel

### ► To cite this version:

Ahmed Nasser Mahgoub, Harald Böhnelt, Claus Siebe, Magdalena Oryaëlle Chevrel. Paleomagnetic study of El Metate shield volcano (Michoacán, Mexico) confirms its monogenetic nature and young age ( 1250 CE). Journal of Volcanology and Geothermal Research, 2017, 336, pp.209 - 218. 10.1016/j.jvolgeores.2017.02.024 . hal-01634724

HAL Id: hal-01634724

<https://uca.hal.science/hal-01634724>

Submitted on 9 Jul 2023

**HAL** is a multi-disciplinary open access archive for the deposit and dissemination of scientific research documents, whether they are published or not. The documents may come from teaching and research institutions in France or abroad, or from public or private research centers.

L'archive ouverte pluridisciplinaire **HAL**, est destinée au dépôt et à la diffusion de documents scientifiques de niveau recherche, publiés ou non, émanant des établissements d'enseignement et de recherche français ou étrangers, des laboratoires publics ou privés.



Distributed under a Creative Commons Attribution - NonCommercial - NoDerivatives 4.0 International License

# Paleomagnetic study of El Metate shield volcano (Michoacán, Mexico) confirms its monogenetic nature and young age (~1250 CE)

Ahmed Nasser Mahgoub<sup>a,\*</sup>, Harald Böhnell<sup>a</sup>, Claus Siebe<sup>b</sup>, Magdalena Oryaëlle Chevrel<sup>c</sup>

<sup>a</sup> Centro de Geociencias, Universidad Nacional Autónoma de México (UNAM), Blvd. Juriquilla No. 3001, Querétaro 76230, Mexico

<sup>b</sup> Departamento de Vulcanología, Instituto de Geofísica, Universidad Nacional Autónoma de México, Coyoacán, C.P. 04510 Ciudad de México, Mexico

<sup>c</sup> Laboratoire Magmas et Volcans, Université Blaise Pascal CNRS, 6 av. Blaise Pascal, 63178 Aubière, France

## ARTICLE INFO

### Article history:

Received 5 December 2016

Received in revised form 10 February 2017

Accepted 26 February 2017

Available online xxxx

### Keywords:

Paleomagnetism

El Metate

Michoacán-Guanajuato Volcanic Field

Holocene secular variation

Paleointensity

Paleomagnetic dating

Monogenetic volcano

## ABSTRACT

In a recent study, Chevrel et al. (2016a, b) radiocarbon-dated the oldest lava flow of the voluminous (~9.2 km<sup>3</sup>) El Metate shield volcano (Michoacán, Mexico) at cal 1250–1260 CE and proposed that its eruption was monogenetic in origin, with twelve younger lava flows emplaced during a short period of only ~35 years, but certainly <275 years. In order to test this hypothesis, we undertook a detailed paleomagnetic study of five lava flows from El Metate to check the consistency of their paleomagnetic directions. Additionally, a group of representative specimens was treated with the double-heating Thellier experiment using the IZZI protocol for paleointensity determination. Flow mean paleomagnetic directions obtained for four of the flows are indistinguishable, and discordant directions were obtained from the site of the 5th flow measured, probably due to the tilting of the sampled block after remanence acquisition. Mean paleodirections and intensities were used for paleomagnetic dating applying the global paleosecular variation model SHA.DIF.14k. The resulting age range for the eruption is 1150–1290 CE, which overlaps with the range previously determined by the <sup>14</sup>C method by Chevrel et al. (2016a). Accepting the <sup>14</sup>C age of the oldest flow as the maximum age, the age range would be reduced to 1250–1290 CE, which strongly supports the hypothesis of a monogenetic nature of the El Metate eruption.

© 2017 Elsevier B.V. All rights reserved.

## 1. Introduction and geological background

El Metate is a shield volcano located in the southern sector of the Michoacán-Guanajuato Volcanic Field (MGVF) and only 14 km NNE of the city of Uruapan in Michoacán, Mexico (Fig. 1). The MGVF forms the western-central section of the Trans-Mexican Volcanic Belt (TMVB), a continental arc that crosses Mexico in an east-west direction between 19° and 21° of northern latitude. The TMVB consists of monogenetic fields, stratovolcanoes, and volcanic plateaus whose distribution is controlled by regional tectonics (e.g. Thorpe, 1977; Ferrari et al., 2012; Johnson and Harrison, 1989; Suter et al., 1999). Its origin is related to the subduction of the Rivera and Cocos plates underneath the North America plate (Pardo and Suárez, 1995). The MGVF contains the largest concentration of monogenetic volcanoes within the TMVB and probably also within a subduction-related volcanic arc in the entire world (Hasenaka and Carmichael, 1985b; Valentine and Connor, 2015). It encloses >1000 monogenetic cinder cones, ~400 medium-sized shields and domes, ~100 isolated viscous flows and lava domes, 22 rare phreatomagmatic structures, and two strato-volcanoes (Hasenaka and Carmichael, 1985a, 1985b, 1987; Hasenaka et al., 1994). The impact of

its two historic monogenetic eruptions of Parícutin (1943–1952) and Jorullo (1759–1774) on human settlements is well documented (Fries, 1953; Luhr and Simkin, 1993; Guilbaud et al., 2011; Rasoazanamparany et al., 2016).

Morphologically, El Metate is characterized by a small roughly symmetrical central dome, which is surrounded by a broad shield of well-preserved young lava flows (Siebe et al., 2014; Chevrel et al., 2016a). It has a basal diameter of ~10 km and a height of ~600 m. Chevrel et al. (2016a, 2016b) proposed that El Metate is composed of thirteen flow units (in stratigraphic order from MT1 to MT13; Fig. 1) and has a total dense rock equivalent volume of 9.2 km<sup>3</sup>.

The first radiocarbon age thought to date El Metate was provided by Hasenaka and Carmichael (1985a) and yielded a conventional date of 4700 ± 200 yr BP. At the same location, Chevrel et al. (2016a) dated the same paleosol and obtained a younger age of 3775 ± 50 yr BP. Through additional field work and with the aid of chemical analyses of the dated ash layer, Chevrel et al. (2016a) discovered that this fallout layer did not stem from El Metate but from the nearby Hoya Urutzen scoria cone. Subsequently, they obtained two new radiocarbon dates on different paleosol samples below the oldest El Metate flow (at site MT1 and 500 m to its east, see Fig. 1), which yielded a combined calibrated age of cal 1250–1260 CE as defined by the overlap at the 95% probability level. They proposed that El Metate was built during one

\* Corresponding author.

E-mail address: ahmednasser@geociencias.unam.mx (A.N. Mahgoub).

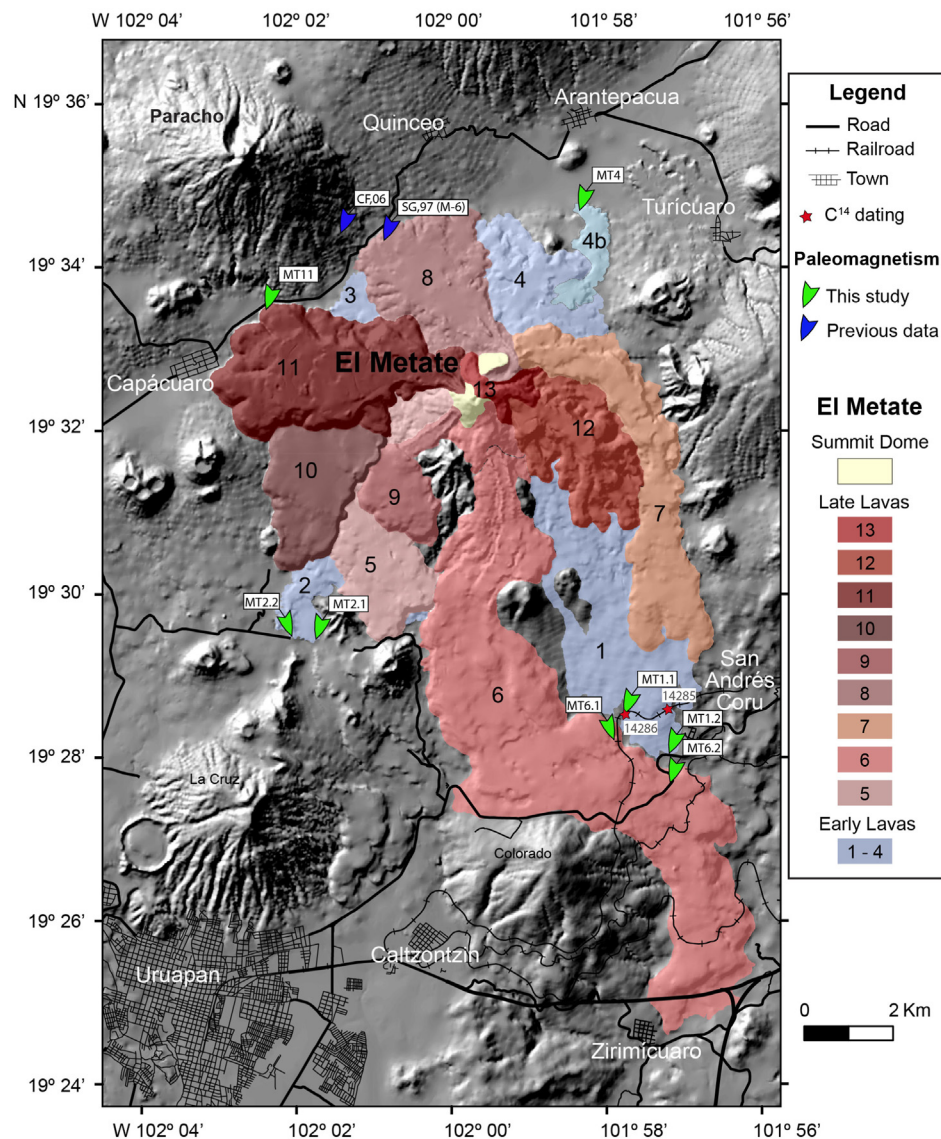


**Fig. 1.** Digital elevation model of El Metate volcano and surroundings with sampling locations (after Chevrel et al., 2016a, 2016b). Thirteen identified lava flows are indicated in colors according to their stratigraphic position. Blue arrows represent the previous paleomagnetic samples SG, 97 (M-6) of Gonzalez et al. (1997), and CF, 06 of Conte-Fasano et al. (2006). Green arrows indicate sampling points of the present paleomagnetic study. Red stars represent the paleosol location for C<sup>14</sup> analysis provided in Chevrel et al. (2016a). (For interpretation of the references to colour in this figure legend, the reader is referred to the web version of this article.)

single eruption and should hence be considered as monogenetic: all thirteen flow units of El Metate (Fig. 1) were erupted during a short time period of possibly ~35 years based on viscosity-based flow velocity estimates, and certainly not longer than 275 years based on historic considerations (the eruption must have ended well before 1530 CE when the Spaniards arrived in this area since the eruption is not mentioned in their chronicles). Unfortunately, no datable material (e.g. paleosol) could be found underneath the stratigraphically youngest lava flows to constrain the duration of the eruption.

The Holocene paleomagnetic secular variation (PSV) database has grown over the recent periods and been used to develop geomagnetic field models like CALS3k.4 (Korte and Constable, 2011), ARCH3k (Korte et al., 2009), and SHA.DIF.14k (Pavón-Carrasco et al., 2014). For such models, data obtained from both heated archeological artifacts and volcanic products certainly are preferred because of their fidelity. During the Holocene, numerous monogenetic eruptions occurred in the MGVF (Hasenaka and Carmichael, 1985a, 1985b; Guilbaud et al., 2012; Siebe et al., 2014; Kshirsagar et al., 2015, 2016; Chevrel et al., 2016a, 2016b) potentially providing a prime source for contributing to the Mexican Holocene PSV database. The last review of PSV data was

published by Böhnel and Molina-Garza (2002), but according to recent, yet unpublished <sup>14</sup>C ages (Siebe, personal information) many of the ages cited in that work are too old, sometimes by several thousands of years. Additionally, sometimes the paleomagnetic data cited there could not be reproduced and thus may be affected by sampling errors, e.g. by selecting unsuitable sites where rocks were moved after cooling or sampling a site that corresponds to a different, undated volcano. Paleointensity data, in particular those obtained several decades ago, might also be unreliable because of the less developed experimental methods used then. We are preparing an update of the PSV data base for Mexico, and in the present work we mention these problems, because they also affected previously published paleomagnetic data for El Metate. During their early attempts in defining the PSV for Mexico, Gonzalez et al. (1997) and Conte-Fasano et al. (2006) conducted paleomagnetic studies on El Metate using the now known to be incorrect age of Hasenaka and Carmichael (1985a, 1985b). Their sampling locations are plotted in Fig. 1, but we note here that the reported coordinates lack precision (reported with only 0.01° or ≈ 1 km resolution). Accordingly, the site of Conte-Fasano et al. (2006) (site CF, 06) plots outside of the area occupied by El Metate lava flows, and site SG, 97 sampled by

Gonzalez et al. (1997) seems to be on top of flow 8, an unlikely location since access to this part is particularly difficult. While both paleomagnetic directions probably correspond to the same El Metate flow (flow 8), as no other lava rocks are exposed within the area around of their reported coordinates, they are discordant between themselves, and also with respect to the directions obtained in this study, obtained from carefully selected sites (Table 1). Altogether this suggests that the paleodirection data published earlier are unreliable, and possibly samples were taken from blocks that were moved after remanence acquisition, which indeed is a serious danger in this blocky lava flow with limited exposures. Only the study of multiple, independent sites as carried out in the present work, may provide reliable paleomagnetic data under such conditions. Gonzalez et al. (1997) also provided a PI of  $52.9 \pm 4.2 \mu\text{T}$ , based on a number of six samples, which still may be reliable as it would at least not be affected by post-cooling movements (see below).

Because of the problems mentioned above we undertook the present study with the goal of determining reliable paleodirections and paleointensities for El Metate lava flows in order to contribute to the PSV data base for Mexico, but also to obtain a paleomagnetic age and compare this with the radiocarbon age of cal 1250–1260 CE provided by Chevrete et al. (2016a). As these authors only could obtain datable material related to the oldest El Metate lava flow, we will test in this work their hypothesis of the monogenetic origin of El Metate and its important consequences for the evolution of this volcano (Chevrete et al., 2016a, 2016b), by studying five lava flows that cover almost the entire stratigraphic section, from the initial to the final stages of the eruption.

## 2. Sampling procedures

Our sampling strategy was designed to define whether El Metate's lava flows were emplaced within a relatively short period (<275 years and possibly only about 35 years) as suggested by Chevrete et al. (2016a), or over a longer time span by several discrete eruptions. Accordingly, during several fieldwork campaigns during the last 12 years, samples were collected from the two oldest lava flows (sites MT1.1 and MT 1.2 for flow 1 and MT2.1 and MT2.2 for flow 2), from two stratigraphically intermediate flows (sites MT4 for flow 4b, and MT6.1 and MT6.2 for flow 6), and from flow 11 (site MT11), which corresponds to the third youngest flow (Fig. 1). The two youngest flows were not sampled because of their difficult access and outcrop

conditions. In MT1, MT2, and MT6, two independent sites were sampled at locations as far as possible from each other (Fig. 1). Within each site, 8 to 16 cores were drilled by using a portable gasoline powered drill with a 25 mm diamond barrel. Cores were between ~8 and 15 cm long and oriented using both magnetic and sun compasses in order to check for local magnetic anomalies (such as produced by lightning strikes). The difference between the magnetic and sun compass readings was on average ~3° and did not exceed 6°. Sampling within each site was distributed laterally as far as possible and aimed at covering a well-averaged area of the flow. Care was taken to ensure that sampling was done on unmoved blocks of rock, as far as this could be assessed in the field; only site MT11 was already suspected during the sampling to be tilted, but since this was the best outcrop that we could find at this flow, we nonetheless decided to give it a try (Fig. 2). Most outcrops were large natural or man-made outcrops, where the interior of the flow could be observed over several tens of meters distance and where no major relative movement of block was apparent. No tilt correction was applied, as all lava flows are unaffected by tectonic movements and unfolded.

In total, 95 cores from five different lava flows were collected. In the laboratory each drill core was cut into specimens of 22 mm length providing at least 3 specimens.

## 3. Rock magnetic properties

Rock magnetic measurements were carried out in samples from each lava flow to define the magneto-mineralogy and thermal stability. Accordingly, on a number of representative specimens, we determined thermomagnetic curves ( $T_{\text{max}} = 600^\circ\text{C}$ ) with a horizontal translation Curie balance in a field of 500 mT, and isothermal remanent magnetization (IRM) acquisition curves.

Thermomagnetic analyses were performed on three cores per lava flow (total 15 samples). Based on the Curie temperatures ( $T_c$ ) defined by the heating curves, the examined samples were categorized into three main groups (Fig. 3). Thereafter, according to the degree of reversibility between the heating and cooling curves, group 1 was split in two subgroups (1a and 1b, Fig. 3). Samples of group 1a (5 cores) are characterized by a single and high Curie temperature  $T_c$  of 530–560 °C with a <10% decrease in magnetization upon cooling to room temperature (Fig. 3a), reflecting the presence of Ti-poor titanomagnetite. All samples of MT11 belong to this group. Group 1b with 3 samples from site MT6 shows a similar behavior (Fig. 3b), but with a stronger decrease of

**Table 1**

(a) Previous and (b) present paleomagnetic site mean directions for El Metate lava flows: SG, 97 of Gonzalez et al. (1997), and CF, 06 of Conte-Fasano et al. (2006), latitude and longitude of the sampling coordinates; n, number of samples used in the calculation of the site-mean direction; N, total number of samples measured; R, unit vector sum; k, precision parameter;  $\alpha_{95}$ , 95% confidence angle; Dec, declination; Inc, inclination. Shaded rows mark rejected sites (see text for details).

Site	Latitude (N)	Longitude (W)	n	N	R	k	$\alpha_{95}$	Dec	Inc
<b>a) Previous studies</b>									
SG, 97	19.57	102.01	5	5	4.98672	301.1	4.4	82.0	41.5
CF, 06	19.57	102.02	8	11	7.99142	816	1.9	16.1	24.6
<b>b) Present study</b>									
<b>Metate 1</b>									
MT1.1	19°28'27.50"	101°57'39.50"	10	12	9.96522	258.80	3.0	355.6	38.5
MT1.2	19°27'57.13"	101°57'8.51"	6	12	5.96926	162.67	5.3	348.7	32.4
Mean			16	24	15.89517	143.09	3.1	352.9	36.2
<b>Metate 2</b>									
MT2.1	19°29'22.01"	102° 1'40.90"	9	12	8.91676	72.20	6.1	349.6	36.0
MT2.2	19°29'26.15"	102° 1'54.88"	6	8	5.92334	65.22	8.4	346.5	32.3
Mean			15	20	14.80145	70.51	4.6	348.4	34.5
<b>Metate 4</b>									
MT4	19°34'39.20"	101°58'12.12"	10	12	9.95519	200.83	3.4	348.5	38.5
<b>Metate 6</b>									
MT6.1	19°28'6.60"	101°57'46.80"	9	12	8.95700	186.05	3.8	348.4	33.8
MT6.2	19°27'39.24"	101°57'5.40"	9	11	8.76939	34.69	8.9	322.3	60.5
<b>Metate 11</b>									
MT11	19°33'30.61"	102° 2'5.20"	13	16	12.89616	115.56	3.9	323.6	71.7
<b>El Metate mean (all samples)</b>			<b>50</b>	<b>95</b>	<b>49.55676</b>	<b>113.10</b>	<b>1.9</b>	<b>349.9</b>	<b>35.7</b>
<b>El Metate mean (site means)</b>			<b>6</b>	<b>8</b>	<b>5.98896</b>	<b>452.95</b>	<b>3.2</b>	<b>349.5</b>	<b>35.3</b>

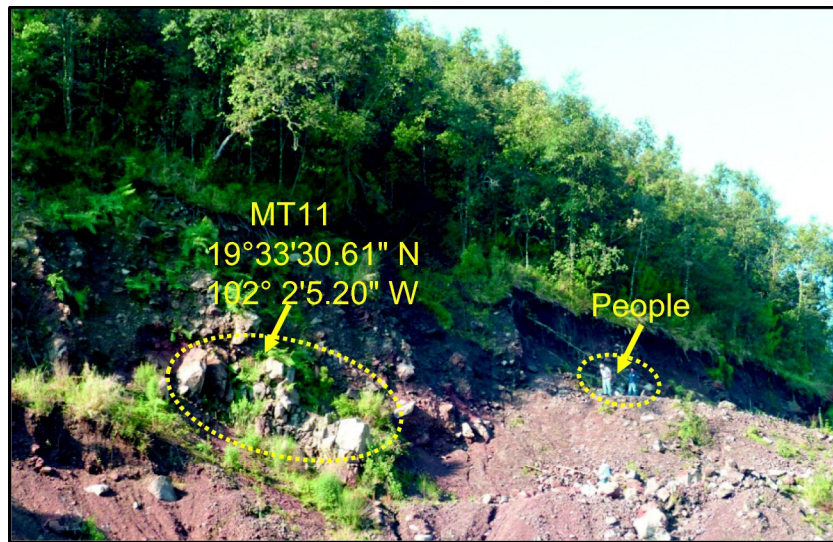


**Fig. 2.** Photograph of sampling site MT11, which is a small quarry excavated into the steep 150-m-high flow front of El Metate's lava flow 11. This was the only outcrop of this flow displaying large blocks (large dashed circle). Unfortunately, we suspect that all blocks at the flow front were moved after cooling, hence useless for our purposes. People (small dashed circle) for scale. The photo was taken facing south.

magnetization after cooling of 10–30%, suggesting an oxidation of the titanomagnetite minerals during heating. Thermomagnetic curves of group 2 (6 samples) show the presence of two magnetic phases with Curie temperatures around 300–330 °C and 500–540 °C interpreted to be both Ti-rich and Ti-poor titanomagnetite minerals, respectively

(Fig. 3c). The cooling curves match with the heating curves reflecting the stability of these minerals against thermal alteration. The three samples of MT2 belong to this group. Finally, group 3 defined by only one sample of MT1 exhibits a similar heating curve (Fig. 3d), but the cooling curve is characterized by the suppression of the low- $T_c$  component and

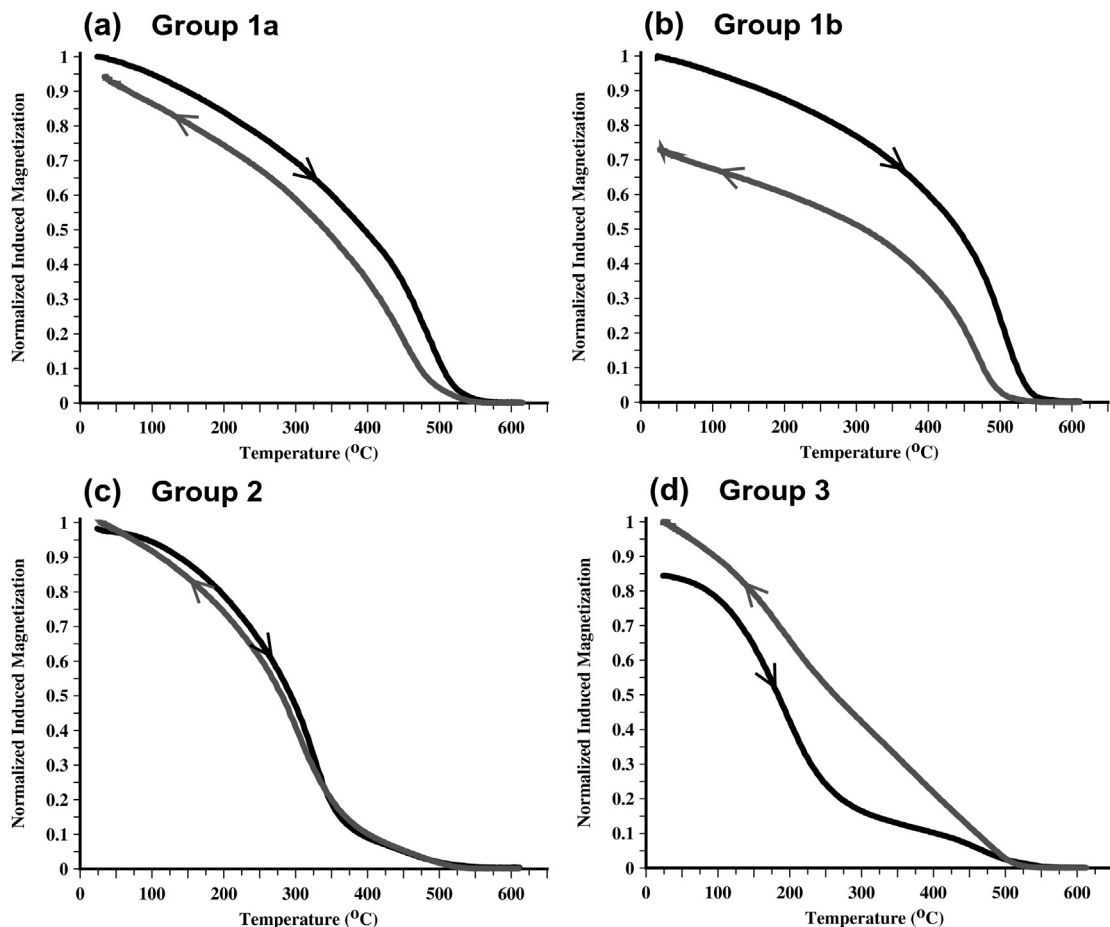


**Fig. 3.** Variation of high-field induced magnetization with temperature showing three groups of thermomagnetic curves, with group 1 subdivided into two subgroups 1a and 1b. Heating and cooling curves are indicated by arrows and black and grey colors, respectively.

is clearly irreversible with a  $\sim 15\%$  increase in magnetization after cooling. This was possibly caused by the exsolution of homogeneous low- $T_c$  titanomagnetite phases to a single phase of Ti-poor titanomagnetite.

Progressive acquisition of IRM in an increasing magnetic field (starting at 10 mT and up to 1000 mT) was done on five cores per flow (total 25). On the basis of their IRM curves, investigated samples were divided into three groups (Fig. 4). Group A was observed in samples from MT1 and MT6 and acquire 90% of their maximum IRM in fields of 0.13–0.16 T, revealing the presence of soft magnetic minerals like magnetite or Ti-poor titanomagnetite probably of pseudo-single domain (PSD) and/or multidomain (MD) grain-sizes. Group B was recognized in both MT2 and MT4 where their IRM saturates at  $\sim 0.3$  T, pointing to the dominance of somewhat higher coercivity (titano-) magnetite minerals of single domain (SD) and/or PSD grain size. MT11 samples belong to group C where IRM reached only 60% of the maximum IRM in fields around 0.2 T and still did not saturate at 0.5 T, thus indicating a contribution of high-coercivity minerals, like SD magnetite or hematite.

#### 4. Paleomagnetic directions

All natural remanent magnetization (NRM) measurements were carried out with an AGICO JR-5 spinner magnetometer (noise level  $\sim 5 \times 10^{-6} \text{ Am}^{-1}$ ). Characteristic remanent magnetization (ChRM) directions were determined by means of stepwise alternating field (AF) demagnetization. For AF demagnetization, an AGICO LDA-3 equipment was used and the samples were demagnetized in 12 steps from 5 to 90 mT. Demagnetization data were analyzed by the program PMGSC 4.2 (Enkin, 2005). From orthogonal vector plots (Fig. 5a, b, c) predominantly univectorial magnetization trends towards the origin of the diagram were observed, sometimes with a small viscous component overprinting the primary one, but this was easily removed at the first steps of AF demagnetization (Fig. 5d, e, f). The median destructive fields (MDFs) for lava flow units 1 and 6 were intermediate (25–30 mT), whereas higher MDFs (40–55 mT) were found in the cooling units 2, 4, and 11. Notably, varying values of MDFs between different cooling units of El Metate reflect their differing magnetic grain sizes. The direction of the ChRM was calculated using principal component analysis (PCA; Kirschvink, 1980). In almost all cases, the ChRM directions for each sample were calculated by 6–10 vector end points and are characterized by maximum angular deviation (MAD) values of  $\sim 1.5^\circ$  on average. Site mean directions were calculated using Fisher statistics (Fisher, 1953, using PMag Tools Version 4.2), after testing for outliers at the 95% confidence level, and are presented in Table 1 and Fig. 6. For lava flows 1

and 2, two sites from each were available to calculate the flow mean directions (Table 1 and Fig. 6a and b). In these flows within-site dispersion was relatively high with a confidence angle  $\alpha_{95}$  between  $6.1$  and  $8.4^\circ$  (except for site MT1.1 which has an  $\alpha_{95} = 3.0^\circ$ ). These sites were taken from railroad cuts and the dispersion may be attributed to small and random movement of blocks along the outcrops. However, it is important to note that all used 31 data points of MT1 and MT2 satisfy the Fisher distribution, as checked applying the appropriate test in the PmagTool program. For MT4, ten samples out of 12 yielded a similar site-mean direction with a low dispersion (Table 1 and Fig. 6c). In regard to cooling unit 6 (MT6), the two sites yielded dissimilar results. For MT6.1, we obtained a well defined site-mean direction with an  $\alpha_{95} = 3.8^\circ$  (Table 1 and Fig. 6d) that is also consistent with the values obtained on the other flows mentioned above. On the other hand, the site mean direction calculated for MT6.2 displays a steep inclination of  $I = 60.5^\circ$  with  $\alpha_{95} = 8.9^\circ$  (Table 1; Fig. 6d), which is different from site MT6.1. This inclination is also inconsistent with the paleosecular variation patterns for central Mexico over the past 4000 years. The reason for this different direction could be undetected block movements, and additionally the inferior rock magnetic properties of these samples, producing the large dispersion. Based on the above, we are confident that MT6.1 represents the El Metate flow MT6 mean direction. Finally, the site-mean direction of MT11 is characterized by a small  $\alpha_{95} = 3.9^\circ$  (Table 1 and Fig. 6e), with a much steeper inclination of  $71.7^\circ$  than the other sites ( $24.6^\circ$  to  $41.5^\circ$ ). As already mentioned above, this result corresponds to one big block exposed at the upper part of the front of flow MT11 (see Fig. 2), which we suspected already during fieldwork to have moved after cooling. Under the reasonable assumption that the block slumped approximately towards the north, this would have produced the inclination difference of about  $35^\circ$ . Site MT11 was therefore not used for further interpretations of paleodirections.

The obtained flow mean directions from lava flows MT1, MT2, MT4, and MT6 were used to evaluate their directional independence by means of the F-distribution test (McFadden and Lowes, 1981). This test shows whether two mean directions are significantly different at a chosen confidence level (in this case 95%). If these directions are indistinguishable they recorded the same field and thus probably represent the same instance in time, in particular for the case of the short age range represented by a volcano such as El Metate. The F-test applied to MT1 and MT6 results in a value of 0.103 which is smaller than the F table value (at 95% significance level) of 0.139, which means that it is positive. Also, the F-test applied to all other flow combinations was positive which indicates that the four flow mean directions of El Metate are undistinguishable at the 95% significance level. Accordingly, an overall El Metate paleodirection was calculated for four flows MT1, MT2, MT4, and MT6 using all individual ChRM directions: Dec =  $349.9$ , Inc =  $35.7$ ,  $n = 50$ , and  $\alpha_{95} = 1.9^\circ$  (Table 1 and Fig. 7a). The mean direction based on six site means is indistinguishable but has a slightly larger confidence angle: Dec =  $349.5$ , Inc. =  $35.3$ ,  $n = 6$ , and  $\alpha_{95} = 3.2^\circ$  (Table 1 and Fig. 7b).

#### 5. Paleointensities

A total of 52 samples were subjected to the double heating Thellier PI experiments (Thellier and Thellier, 1959) applying the IZZI protocol (Tauxe and Staudigel, 2004). In this protocol the Aitkin in-field/zero-field (Aitken et al., 1988; IZ) and the Coe zero-field/in-field (Coe, 1967; ZI) protocols are applied consecutively, which allows to detect the effect of high temperature pTRM tails (Yu and Tauxe, 2005; Yu et al., 2004). Both pTRM (Coe, 1967) and pTRM-tail checks (Riisager and Riisager, 2001) were used to check for alteration of magnetic minerals. For the experiments we used an ASC Scientific TD48 furnace, with heating steps of 100, 200, 250, 300, 340, 370, 400, 430, 460, 490, 510, 530, 560, and  $580^\circ\text{C}$ . pTRM checks were done at 100, 250, 340, 400, 460, and  $510^\circ\text{C}$  while pTRM-tail checks at 250, 340, 400, 460, 510, and  $560^\circ\text{C}$ . For 25 cylindrical samples (group 1) the laboratory field of

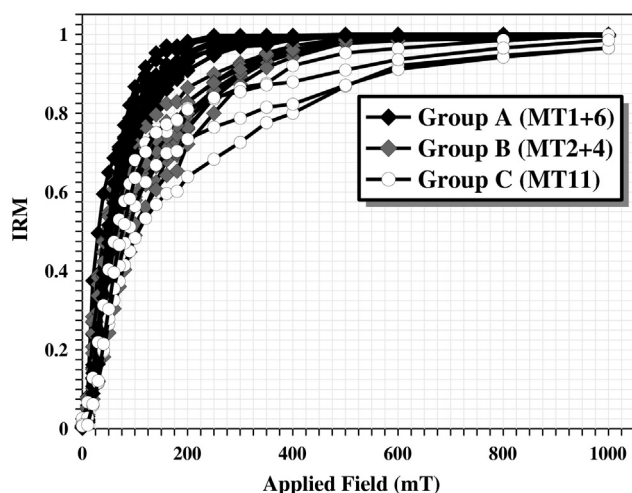


Fig. 4. Normalized IRM acquisition curves for three groups of samples.

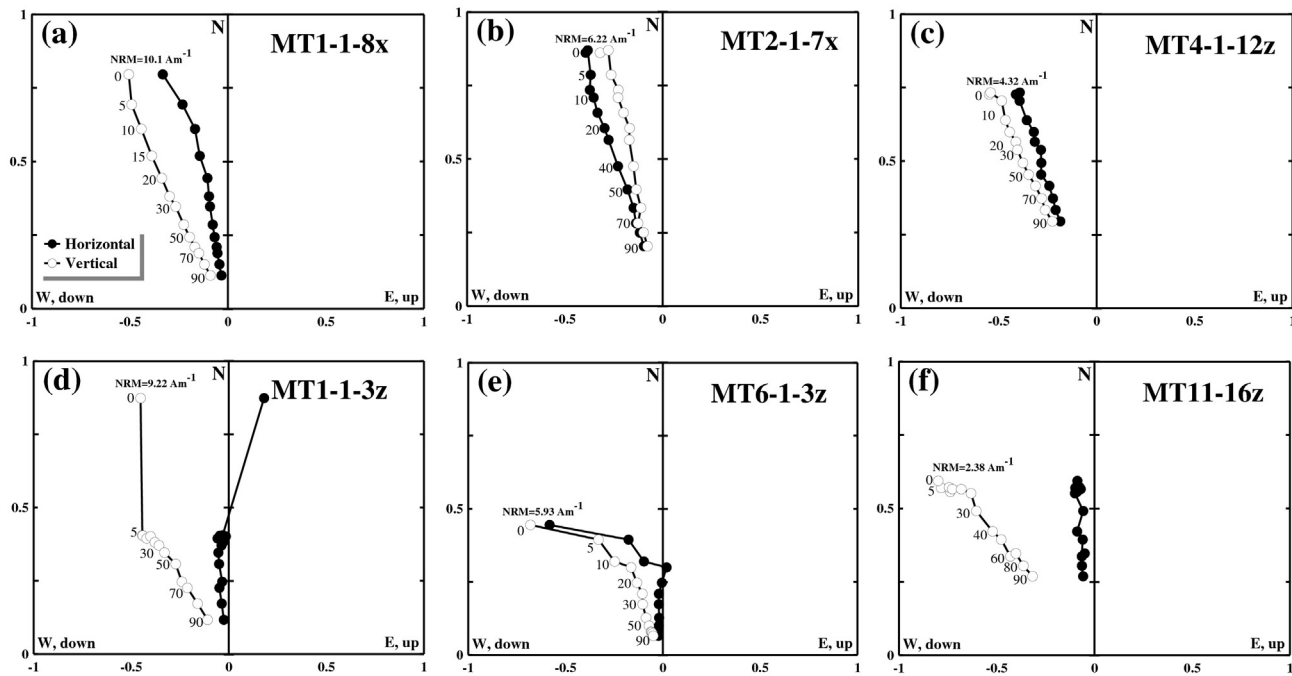


Fig. 5. Orthogonal vector plots of AF demagnetized samples from the five studied lava flows. Labels along curves denote the maximum AF amplitude applied during the demagnetization steps.

60  $\mu\text{T}$  was applied parallel to their z-axis, while for a second group (group 2) of 27 samples their NRM directions were oriented parallel to the applied field (60  $\mu\text{T}$ ) with a precision better than  $5^\circ$ . For PI experiments only samples with a single-component NRM were selected.

Data were analyzed with the ThellierTool4.11 software (Leonhardt et al., 2004), and in order to evaluate our PI estimates the acceptance criteria sets A and B as given in the Thellier tool (Leonhardt et al., 2004) and with the modifications of Paterson et al. (2014; TTA and TTB) were used (for more details see <http://www.paleomag.net/SPD/home.html>). Furthermore, at the flow level, at least three specimens should be available to calculate the flow mean intensity with a standard deviation ( $\sigma$ ) either  $<20\%$  or smaller than 10  $\mu\text{T}$ .

Paleointensity results for each studied flow are listed in Table 2 together with different quality parameters, and representative PI or Arai plots are shown in Fig. 8a. In total, 27 specimens passed the Thellier Tool A or B acceptance criteria resulting in an overall success rate of 52%. We note that the success rate varies for the samples according to

their orientation with respect to the applied field, with  $\sim 40\%$  for group 1 (with the applied field parallel to the sample's z-axis) and  $\sim 63\%$  for group 2 (with the field direction parallel to the sample's NRM). Predominantly, failure was due to multi-domain effects, which is clearly visible in the Arai plots as 'zigzagging' or 'sagging' (Fig. 8b). In regard to flow MT4, six specimens gave a mean PI of  $43.44 \pm 14.02$  with a standard deviation that is larger than the maximum allowed value of 10  $\mu\text{T}$  and thus this PI estimate was excluded from further discussion. For the remaining flows, three to seven specimens passed the acceptance criteria and their PI were used to calculate the flow mean PI (Table 2), with standard deviations ranging between 8.51 and 4.38  $\mu\text{T}$ .

In order to ascertain whether the mean-PI values for El Metate lava flows are similar, a two-sample Student's *t*-test assuming equal variance and using a pooled estimate of the variance  $\mu$  was performed. In this test the null hypothesis stating that the two means are equal ( $H_0: \mu_1 = \mu_2$ ) is checked against the alternative hypothesis that the two means are different ( $H_a: \mu_1 \neq \mu_2$ ). Our analyses confirm the null hypothesis, since

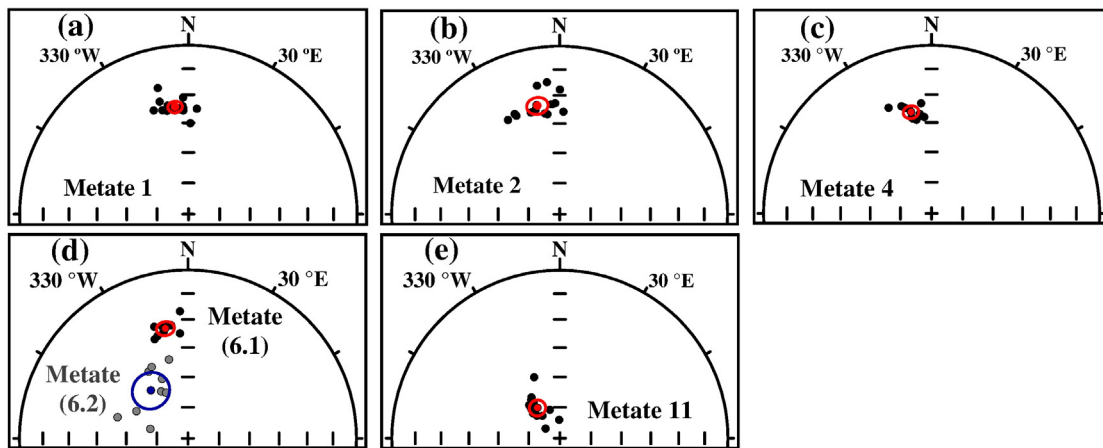
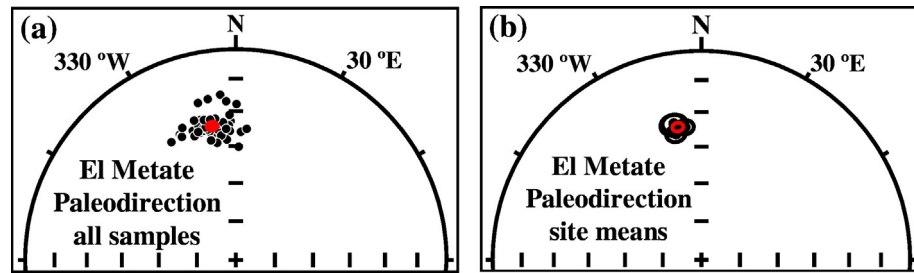


Fig. 6. Characteristic remanent magnetization directions for the five lava flows. Flow mean directions are shown by larger red dots and their 95% confidence angles. Metate site 6.2 directions are distinguished from site 6.1 by grey colour and its mean by blue colour (for more information see text). (For interpretation of the references to colour in this figure legend, the reader is referred to the web version of this article.)



**Fig. 7.** (a) Overall mean direction for El Metate based on all individual samples, shown by the red dot and red 95% confidence angle. (b) Site mean directions of four El Metate lava flows with 95% confidence angles and the resulting mean direction shown in red colour. (For interpretation of the references to colour in this figure legend, the reader is referred to the web version of this article.)

the  $t$ -value of 0.377 is less than the 95% confidence level of 2.228, when comparing MT1 with MT11. Similarly, comparing MT1 with MT2 and MT1 with MT6 provides comparable  $t$ -test results, showing that these flow mean PI are concordant as well. Thus, 21 accepted PI data from flows MT1, MT2, MT6, and MT11 were used to calculate an overall mean paleointensity of  $55.58 \pm 6.64 \mu\text{T}$  (Table 2) for El Metate volcano.

## 6. Paleomagnetic dating

Using the full vector paleomagnetic result for El Metate, we applied the paleomagnetic dating method to this volcano by means of the

Matlab tool *archaeo\_dating* (Pavón-Carrasco et al., 2011). The global field model SHA.DIF.14k (Pavón-Carrasco et al., 2014) was used to accomplish this task. Recently, this model was successfully applied on two lava flows from Ceboruco volcano in western Mexico (Böhnel et al., 2016), which is of a similar age as El Metate. As input data for the paleomagnetic dating, we may use the overall mean of the six accepted site mean directions (Table 1). These directions are characterized by variable sample numbers and dispersion, as reflected by precision parameters  $k$  with values between 65.22 and 258.80. To avoid a bias of the overall mean direction by data of lower precision, a weighting of these site mean directions would be necessary, which is not commonly done. Therefore, we used the overall mean based on the listed site mean

**Table 2**

The Thellier–IZZI paleointensity results and associated statistics: Field direction, arb/par, arbitrary along z-axis, parallel to the sample NRM; N, number of points included in the linear best-fit;  $f$ , fraction of the NRM used for best-fit;  $g$ , the gab factor;  $q$ , quality factor; MAD<sub>anc</sub>, anchored maximum angular deviation;  $\alpha$ , angular difference between anchored and non-anchored best solution;  $\delta\text{CK}$ , relative check error;  $\delta\text{pal}$ , cumulative check difference;  $\delta\text{TR}$ , tail check;  $\delta t^*$ , normalized tail of pTRM; PI, paleointensity;  $\sigma$  ( $\mu\text{T}$ ), standard deviation.

Sample	Field direction	N	T (°C)	f	g	q	MAD <sub>anc</sub>	$\alpha$	$\delta\text{CK}$	$\delta\text{pal}$	$\delta\text{TR}$	$\delta t^*$	Class	PI	$\sigma$ ( $\mu\text{T}$ )
<b>Metate 1 (MT1)</b>															
2b	arb	6	0–340	0.82	0.74	6.31	3.14	1.89	5.37	10.85	5.92	6.26	B	53.04	5.23
3z	par	12	200–560	0.47	0.87	6.89	4.25	14.7	3.51	1.41	1.89	1.75	A	48.58	2.86
4b	par	6	0–340	0.72	0.75	24.4	2.30	2.32	3.41	2.98	5.21	7.54	A	51.00	1.13
5z	par	6	100–370	0.62	0.67	26.8	2.22	2.98	6.28	6.67	3.23	4.25	A	50.88	0.79
6b	par	12	0–510	0.72	0.88	23.3	2.91	6.21	8.87	3.54	3.91	2.54	B	63.11	1.72
7b	par	13	0–530	0.86	0.85	13.0	5.09	6.91	8.57	4.21	3.12	1.54	B	50.42	2.83
10z	arb	6	0–340	0.76	0.77	7.30	2.00	1.65	2.63	1.16	7.04	4.62	A	58.10	4.64
Mean														53.59	5.17
<b>Metate 2 (MT2)</b>															
2z	arb	12	0–510	0.81	0.80	11.0	3.22	2.87	3.60	9.10	2.08	3.97	A	68.50	4.05
7z	par	13	0–530	0.40	0.75	2.62	2.57	10.8	4.99	5.97	7.96	4.43	B	58.44	6.45
12a	par	9	0–430	0.47	0.77	4.90	2.73	7.55	1.80	3.07	1.43	1.90	B	54.98	4.12
Mean														60.64	7.02
<b>Metate 4 (MT4)</b>															
4a	par	10	0–460	0.44	0.87	4.51	3.62	8.74	3.85	11.7	4.82	3.62	B	32.59	2.79
6z	arb	9	0–430	0.40	0.79	2.71	3.31	9.06	6.52	0.94	0.67	13.8	B	41.81	4.81
7z	arb	9	0–430	0.48	0.83	4.84	3.72	8.80	2.68	2.37	4.44	5.51	B	31.93	2.62
10a	par	12	0–510	0.55	0.82	5.30	2.05	3.37	2.25	2.68	2.18	2.87	A	54.99	4.70
11z	arb	7	0–370	0.47	0.78	5.30	3.60	6.13	3.65	5.45	3.14	2.46	A	33.56	2.30
12z	arb	12	0–510	0.69	0.79	8.71	1.73	1.71	2.02	5.73	3.29	1.41	A	65.78	4.13
Mean														43.44	14.02
<b>Metate 6 (MT6)</b>															
1a	par	12	0–510	0.71	0.78	7.77	1.59	0.31	3.45	1.48	3.24	4.41	A	68.53	4.88
3a	arb	6	100–370	0.42	0.77	3.43	5.0	6.84	8.21	9.14	4.02	5.31	B	42.37	4.00
7b	par	12	0–510	0.79	0.86	10.7	4.89	6.97	6.92	0.66	7.78	1.26	A	50.53	3.20
8z	arb	8	0–400	0.40	0.75	2.36	1.93	4.50	5.96	11.75	3.0	0.30	B	60.50	7.70
9a	par	6	0–340	0.42	0.77	3.73	2.52	0.92	5.05	0.36	2.57	5.60	B	61.85	5.41
10z	par	13	100–560	0.88	0.82	11.2	2.11	1.86	4.91	3.21	4.53	1.56	A	53.20	3.41
Mean														56.16	8.51
<b>Metate 11 (MT11)</b>															
2b	par	14	0–560	0.37	0.87	4.22	1.65	2.67	6.35	4.24	4.38	6.07	B	61.39	4.36
5z	par	10	300–560	0.41	0.76	7.35	1.98	3.0	3.87	7.59	2.10	3.97	B	56.23	2.41
7z	Arb	12	200–560	0.91	0.83	28.2	3.74	2.92	4.83	6.13	3.14	2.39	A	53.53	1.42
14b	par	9	100–460	0.55	0.75	10.6	5.04	14.5	6.09	6.05	2.99	1.56	A	51.79	2.04
16b	par	14	0–560	0.82	0.91	41.3	5.89	7.26	4.76	5.42	1.39	0.26	A	50.23	0.91
Mean														54.63	4.38

El Metate Paleointensity: PI = 55.58;  $\sigma$  = 6.64;  $n$  = 21.

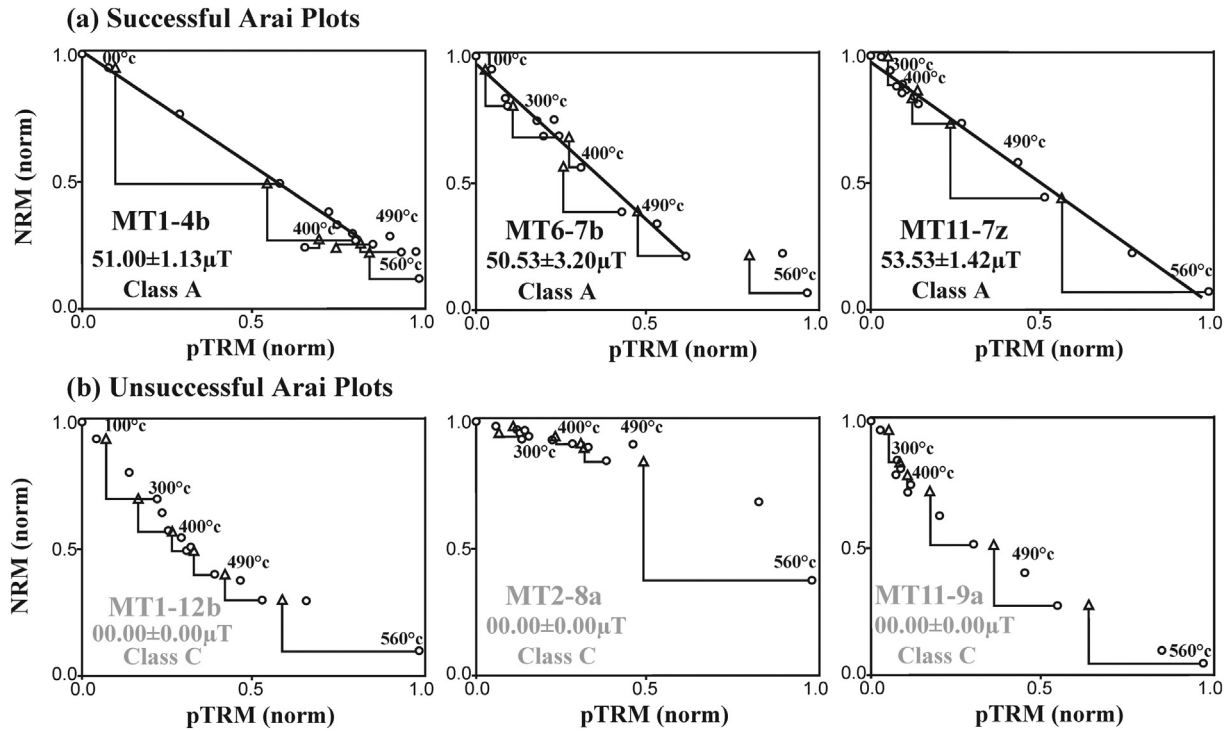


**Fig. 8.** IZZI-Thellier results. (a) Three examples of typical IZZI-Thellier results passing the two defined sets of selection criteria; A and B class. (b) Three examples of rejected IZZI-Thellier results which accordingly affiliated to C class. NRM and pTRM are normalized. NRM vs. pTRM data are shown as circles, with the black best-fit lines. pTRM checks are shown as triangles. Some temperature steps also indicated. The analyses were done using TellierTool.

directions. On the other hand, we have shown above that all site mean directions are indistinguishable, suggesting a very similar age. We therefore will use the overall mean direction calculated from 52 ChRM directions from all accepted sites as our main choice for dating.

As the oldest El Metate lava flow MT1 has a maximum radiocarbon age of about cal 1150 CE (see [Chevrel et al., 2016a](#)) and could not be

younger than the arrival of the Spaniards around 1550 CE, we restricted the time interval to this period 1150–1550 CE. This provides a well constrained paleomagnetic age range of 1150–1290 CE ([Fig. 9](#)), which coincides well with the calibrated radiocarbon age. Using the paleodirection based on the site mean directions, this age range would only increase by nine years to 1150–1299 CE.

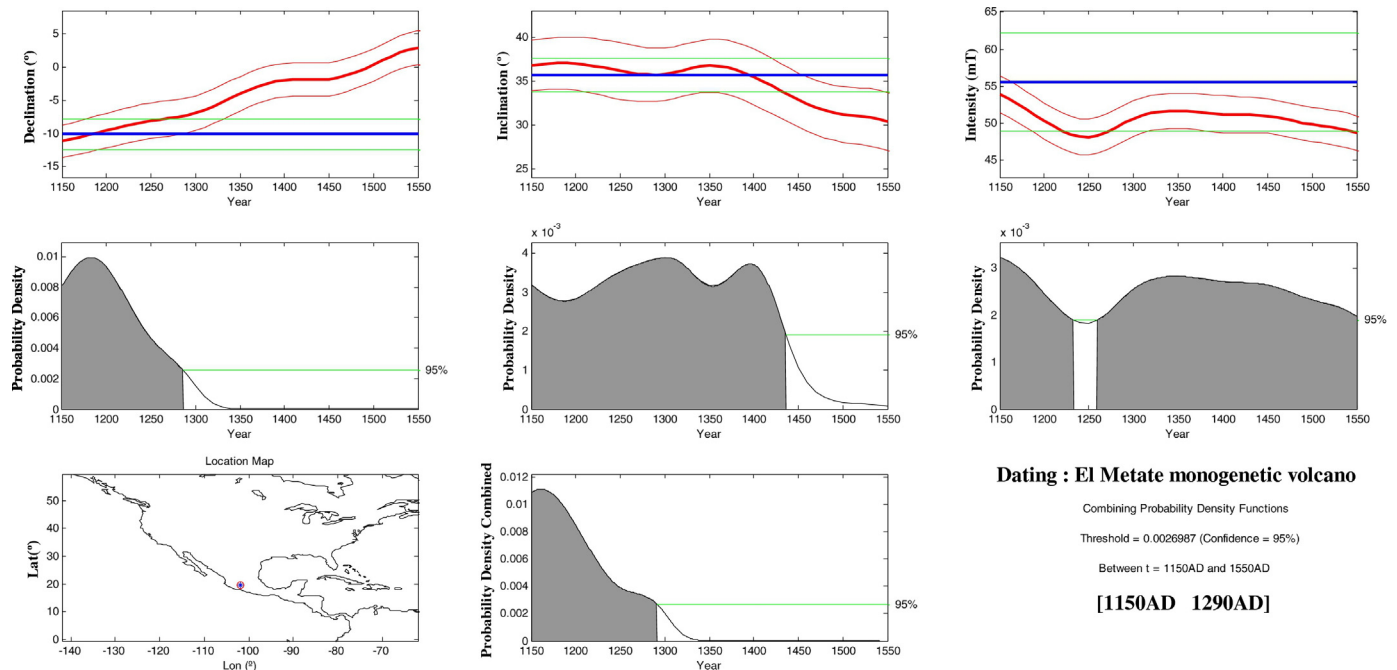


**Fig. 9.** Paleomagnetic dating of El Metate monogenetic shield volcano. Red curves show the variation in time of the components of the paleomagnetic field as determined from the SHA.DIF.14k model, and blue horizontal lines are the components of the full vector direction determined for El Metate volcano; all curves and lines are shown with their respective 95% confidence intervals. The combined probability density derived from the declination, inclination, and paleointensity data is shown as shaded peaks and the minimum 95% confidence level by horizontal green lines. (For interpretation of the references to colour in this figure legend, the reader is referred to the web version of this article.)

## 7. Discussion: are the El Metate lava flows the result of one single or several independent eruptions?

Rock magnetic properties obtained from thermomagnetic analyses and IRM acquisition curves revealed differences between the five lava flows of El Metate shield volcano pointing to variations in the composition and size of magnetic particles in these flows. Such variations are to be expected, since El Metate erupted two compositionally different types of magma (Chevrel et al., 2016b). This magma variability together with different cooling histories of the sampling sites of the El Metate flows, as well as their sampling at certainly different levels within these flows may explain the variations in magnetic mineralogy and grain sizes.

Our study covered the entire stratigraphy of lava flows accessible in the field (MT1 to MT11), and wherever possible, two or more independent sites were sampled in order to check the within-flow paleomagnetic consistency (e.g. Hagstrum and Champion, 1994; Speranza et al., 2006; Böhnelt et al., 2016). Good quality site mean directions were obtained from the eight studied sites, but MT6.2 and MT11 had to be rejected because their mean direction differed strongly from other sites of the same flow. The remaining paleodirections from flows MT1, MT2, MT4, and MT6 are very consistent and indistinguishable at the 95% confidence level, allowing to combine all ChRM directions into one overall mean direction. This direction is interpreted to represent the geomagnetic field during the buildup of El Metate volcano, and the indistinguishable directions of the different flows suggest that they were all erupted during a short time period of probably <50–100 years, as otherwise the secular variation would have resulted in the acquisition of significantly different directions (for typical secular variation changes during the last 21 centuries, see for example Bucur, 1994).

Concordant and reliable IZZI-Thellier results were obtained from four out of five lava flows, and the success rate at the sample level was 52% and thus relatively high. Our PI results support the suggestion of Paterson et al. (2015) and De Groot et al. (2016) that choosing a small angle between the applied field direction and the sample NRM during paleointensity experiments reduces the multi-domain effect and thus enhances the technical quality of the PI results. This is clearly shown by our samples, with a success rate of 63% for the group where the field was parallel to the NRM direction vs. 40% for the group with a random angular orientation.

The concordant paleodirections and paleointensities of the studied lava flows indicate that they were emplaced during a period of <50–100 years, which thus supports the monogenetic origin of El Metate shield volcano as proposed by Chevrel et al. (2016a, 2016b). It must be noted however that the paleomagnetic dating method can inherently not determine a shorter emplacement period than 100–200 years for El Metate, due to the uncertainty of the used field model SHA.DIF.14k and the uncertainty of the paleomagnetic results. Even so, the youngest possible age defined by the arrival of the Spanish conquerors to the El Metate area in 1530 CE can be excluded by the paleomagnetic age range of 1150–1290 CE. This range overlaps entirely the  $^{14}\text{C}$  age range as defined by its error limits. If we use the age proposed by Chevrel et al. (2016a) as the most probable for flow MT1 (cal 1250–1260 CE) as a limit for the paleomagnetic age range, only a short period of 40 years would remain for the emplacement of the younger lava flows. This is in very good agreement with the eruption time of about 35 years proposed by Chevrel et al. (2016a), based on a total emitted lava volume of 10.8 km<sup>3</sup> and a continuous extrusion rate of 10 m<sup>3</sup>/s.

Our results are derived from a completely independent dating method, which also applies to the previous undated younger El Metate flows. They strongly support the hypothesis of Chevrel et al. (2016a, 2016b) that this huge volcano indeed is not a common shield or composite volcano with a prolonged eruption history. For the consequences of such a short eruption time representing in terms of magma composition and evolution, eruption style, and magma viscosity, we refer to their original publications.

## 8. Conclusions

The present study supports that El Metate is the youngest (cal 1250–1260 CE) monogenetic shield volcano of the Michoacán–Guanajuato Volcanic Field, and with a total volume of ~9.2 km<sup>3</sup> the most voluminous Holocene eruption in Mexico and the most voluminous andesitic effusive eruption worldwide so far reported as proposed by Chevrel et al. (2016a, 2016b). Five of thirteen lava flows from this shield volcano were studied by rock-magnetic, paleomagnetic, and paleointensity methods in order to test its monogenetic origin, as only the oldest flow could be  $^{14}\text{C}$  dated. Flow-mean paleomagnetic directions obtained from four flows (MT1, MT2, MT4, and MT6) are indistinguishable, and the only discordant mean direction available for site MT11 is certainly due to block movement after remanence acquisition. Similar problems were also found in a few sites from other flows. Such discordant results show that it is mandatory to ensure that the sampled lava blocks are in place, and if possible to core multiple sites along each of the lava flows, especially when these are of such great thickness and extremely blocky in nature as it is the case of El Metate. Flow mean directions are indistinguishable at the 95% confidence level and suggest that these flows were emplaced in a time span of probably <50–100 years, which is further supported by concordant flow-mean paleointensity values obtained from four flows. Paleomagnetic dating of El Metate volcano indicates an age range between 1150–1290 CE (95% probability level) and thus confirms its  $^{14}\text{C}$  age of 1250–1260 CE. Using this most probable  $^{14}\text{C}$  age as a limit for the paleomagnetic dating, this restricts the duration of the eruption to only 40 years, ending much before the first arrival of the Spanish conquerors around 1530 CE. Thus we conclude that the paleomagnetic data are fully compatible with a monogenetic origin of El Metate volcano. Interestingly, if small scoria cone eruptions are known to have important repercussions (e.g. Parícutin), much more voluminous shield volcanoes such as El Metate should have an even larger impact on the local population and environment, possibly triggering human migrations (Chevrel et al., 2016a). Unfortunately, El Metate's impact is still difficult to evaluate in the absence of written sources from archeological sites (Pereira et al., 2013).

## Acknowledgments

Ing. J. Escalante supported studies with the Curie balance and Ing. Emilio Nava the maintenance of the computers and network in the laboratory. Field and laboratory costs of A.N.M. and H.B. were covered by Consejo Nacional de Ciencia y Tecnología funds (CONACyT-180032) and those of O.C. and C.S. were defrayed from projects CONACyT-167231 and the Dirección General de Asuntos del Personal Académico (DGAPA, UNAM IN-101915) granted to C. Siebe. We thank Américo González-Esparza, Adriana Briseño, and Ernesto Andrade at UNAM Campus Morelia for providing lodging facilities at the Mexican Array Radio Telescope (MEXART) near Coeneo during field campaigns.

## References

- Aitken, M.J., Allsop, A.L., Bussell, G.D., Winter, M.B., 1988. Determination of the intensity of the Earth's magnetic field during archaeological times—reliability of the Thellier technique. *Rev. Geophys.* 26, 3–12.
- Böhnelt, H., Molina-Garza, R., 2002. Secular variation in Mexico during the last 40,000 years. *Phys. Earth Planet. Inter.* 133 (1), 99–109.
- Böhnelt, H., Pavón-Carrasco, F.J., Sieron, K., Mahgoub, A.N., 2016. Palaeomagnetic dating of two recent lava flows from Ceboruco volcano, western Mexico. *Geophys. J. Int.* 207 (2), 1203–1215.
- Bucur, I., 1994. The direction of the terrestrial magnetic field in France during the last 21 centuries. *Phys. Earth Planet. Inter.* 87, 95–109.
- Chevrel, M.O., Siebe, C., Guilbaud, M.N., Salinas, S., 2016a. The 1250 CE El Metate shield (Michoacán): Mexico's most voluminous Holocene eruption and its significance for archaeology and hazards. *The Holocene* 26 (3):471–488. <http://dx.doi.org/10.1177/0959683615609757>.
- Chevrel, M.O., Guilbaud, M.N., Siebe, C., 2016b. The AD 1250 effusive eruption of El Metate shield volcano (Michoacán, Mexico): magma source, crustal storage, eruptive dynamics, and lava rheology. *Bull. Volcanol.* 78 (4):32. <http://dx.doi.org/10.1007/s00445-016-1020-9>.

- Coe, R.S., 1967. Paleo-intensities of the Earth's magnetic field determined from Tertiary and Quaternary rocks. *J. Geophys. Res.* 72 (12), 3247–3262.
- Conte-Fasano, G., Urrutia-Fucugauchi, J., Goguitaichivili, A., Morales-Contreras, J., 2006. Low-latitude paleosecular variation and the time-averaged field during the late Pliocene and Quaternary—paleomagnetic study of the Michoacan-Guanajuato volcanic field, Central Mexico. *Earth Planets Space* 58 (10), 1359–1371.
- Enkin, R., 2005. PMGSC 4.2, Geological Survey of Canada, Sidney, British Columbia, Canada.
- Ferrari, L., Orozco-Esquivel, T., Manea, V., Manea, M., 2012. The dynamic history of the Trans-Mexican Volcanic Belt and the Mexico subduction zone. *Tectonophysics* 522, 122–149.
- Fisher, R.A., 1953. Dispersion on a sphere. *Proc. R. Soc. Lond. A* 127, 205–305.
- Fries, C., 1953. Volumes and weights of pyroclastic material, lava and water erupted by Parícutin Volcano, Michoacan, Mexico. *Trans. Am. Geophys. Union* 34, 603–616.
- Gonzalez, S., Sherwood, G., Böhnell, H., Schnepf, E., 1997. Paleosecular variation in Central Mexico over last 30,000 years: the record from lavas. *Geophys. J. Int.* 130, 201–219.
- de Groot, L.V., Pimentel, A., Di Chiara, A., 2016. The multimethod palaeointensity approach applied to volcanics from Terceira: full-vector geomagnetic data for the past 50 kyr. *Geophys. J. Int.* 206 (1), 590–604.
- Guilbaud, M.N., Siebe, C., Layer, P., Salinas, S., Castro-Govea, R., Garduño-Monroy, V.H., Le Corvec, N., 2011. Geology, geochronology, and tectonic setting of the Jorullo Volcano region, Michoacán, México. *J. Volcanol. Geotherm. Res.* 201:97–112. <http://dx.doi.org/10.1016/j.jvolgeores.2010.09.005>.
- Guilbaud, M.N., Siebe, C., Layer, P., Salinas, S., 2012. Reconstruction of the volcanic history of the Tacámbaro-Puruarán area (Michoacán, México) reveals high frequency of Holocene monogenetic eruptions. *Bull. Volcanol.* 74, 1187–1211.
- Hagstrum, J.T., Champion, D.E., 1994. Paleomagnetic correlation of Late Quaternary lava flows in the lower east rift zone of Kilauea Volcano, Hawaii. *J. Geophys. Res.* 99, 21679–21690.
- Hasenaka, T., Carmichael, I.S.E., 1985a. The cinder cones of Michoacán-Guanajuato, central Mexico: their age, volume and distribution, and magma discharge rate. *J. Volcanol. Geotherm. Res.* 25, 105–124.
- Hasenaka, T., Carmichael, I.S.E., 1985b. Compilation of location, size, and geomorphological parameters of volcanoes of the Michoacán-Guanajuato volcanic field, central Mexico. *Geophys. Int.* 24 (4), 577–607.
- Hasenaka, T., Carmichael, I.S.E., 1987. The cinder cones of Michoacán-Guanajuato, central Mexico: petrology and chemistry. *J. Petrol.* 28, 241–269.
- Hasenaka, T., Ban, M., Delgado-Granados, H., 1994. Contrasting volcanism in the Michoacán-Guanajuato volcanic field, central Mexico: shield volcanoes vs. cinder cones. *Geophys. J. Int.* 33 (1), 125–138.
- Johnson, C.A., Harrison, C.G.A., 1989. Tectonics and volcanism in central Mexico: a Landsat thematic mapper perspective. *Remote Sens. Environ.* 28, 273–286.
- Kirschvink, J.L., 1980. The least-squares line and plane and analysis of palaeomagnetic data. *Geophys. J. R. Astron. Soc.* 62, 699–718.
- Korte, M., Constable, C., 2011. Improving geomagnetic field reconstructions for 0–3 ka. *Phys. Earth Planet. Inter.* 188 (3), 247–259.
- Korte, M., Donadini, F., Constable, C.G., 2009. Geomagnetic field for 0–3 ka: 2. A new series of time-varying global models. *Geochim. Geophys. Geosyst.* 10.
- Kshirsagar, P., Siebe, C., Guilbaud, M.N., Salinas, S., Layer, P., 2015. Late Pleistocene Alberca de Guadalupe maar volcano (Zacapu basin, Michoacán): stratigraphy, tectonic setting, and paleo-hydrogeological environment. *J. Volcanol. Geotherm. Res.* 304: 214–236. <http://dx.doi.org/10.1016/j.jvolgeores.2015.09.003>.
- Kshirsagar, P., Siebe, C., Guilbaud, M.N., Salinas, S., 2016. Geological and environmental controls on the change of eruptive style (phreatomagmatic to Strombolian-effusive) of Late Pleistocene El Caracol tuff cone and its comparison with adjacent volcanoes around the Zacapu basin (Michoacán, México). *J. Volcanol. Geotherm. Res.* 318: 114–133. <http://dx.doi.org/10.1016/j.jvolgeores.2016.03.015>.
- Leonhardt, R., Heunemann, C., Krása, D., 2004. Analyzing absolute paleointensity determinations: acceptance criteria and the software ThellierTool4.0. *Geochim. Geophys. Geosyst.* 5 (12).
- Luhr, J.F., Simkin, T., 1993. Parícutin. The Volcano Born in a Mexican Cornfield. Geoscience Press, Phoenix, Arizona 427 p.
- McFadden, P.L., Lowes, F.J., 1981. The discrimination of mean directions drawn from Fisher distributions. *Geophys. J. R. Astron. Soc.* 67, 19–33.
- Pardo, M., Suárez, G., 1995. Shape of the subducted Rivera and Cocos plates in southern Mexico: seismic and tectonic implications. *J. Geophys. Res.* 100 (12), 12,357–12,373.
- Paterson, G.A., Tauxe, L., Biggin, A.J., Shaar, R., Jonestrask, L.C., 2014. On improving the selection of Thellier-type paleointensity data. *Geochim. Geophys. Geosyst.* 15, 1180–1192.
- Paterson, G.A., Biggin, A.J., Hodgson, E., Hill, M.J., 2015. Thellier-type paleointensity data from multidomain specimens. *Phys. Earth Planet. Inter.* 245:117–133. <http://dx.doi.org/10.1016/j.pepi.2015.06.003>.
- Pavón-Carrasco, F.J., Rodríguez-González, J., Ossete, M.L., Torta, J.M., 2011. A Matlab tool for archaeomagnetic dating. *J. Archaeol. Sci.* 38, 408–419.
- Pavón-Carrasco, F.J., Ossete, M.L., Torta, J.M., De Santis, A., 2014. A geomagnetic field model for the Holocene based on archaeomagnetic and lava flow data. *Earth Planet. Sci. Lett.* 388, 98–109.
- Pereira, G., Michelet, D., Migeon, G., 2013. La migración de los purépecha hacia el norte y su regreso a los lagos. *Arqueol. Mex.* 21 (123), 55–60.
- Rasoazanampanary, C., Widom, E., Siebe, C., Guilbaud, M.N., Spicuzza, M.J., Valley, J.W., Valdez, G., Salinas, S., 2016. Temporal and compositional evolution of Jorullo volcano, Mexico: implications for magmatic processes associated with a monogenetic eruption. *Chem. Geol.* 434:62–80. <http://dx.doi.org/10.1016/j.chemgeo.2016.04.004>.
- Risager, P., Risager, J., 2001. Detecting multidomain magnetic grains in Thellier paleointensity experiments. *Phys. Earth Planet. Inter.* 125 (1), 111–117.
- Siebe, C., Guilbaud, M.N., Salinas, S., Kshirsagar, P., Chevrel, M.O., De la Fuente, J.R., Hernández-Jiménez, A., Godínez, L., 2014. Monogenetic volcanism of the Michoacán-Guanajuato Volcanic Field: Maar craters of the Zacapu basin and domes, shields, and scoria cones of the Tarascan highlands (Parícutin region). *Field Guide, Pre-meeting Fieldtrip for the 5th International Maar Conference (5IMC-IAVCEI)*, Querétaro, 13–17 November, México 33 p.
- Speranza, F., Branca, S., Coltelli, M., D'Ajello Caracciolo, F., Vigliotti, L., 2006. How accurate is "paleomagnetic dating"? New evidence from historical lavas from Mount Etna. *J. Geophys. Res.* Solid Earth 111 (B12). <http://dx.doi.org/10.1029/2006JB004496>.
- Suter, M., Contreras, J., Gómez-Tuena, A., Siebe, C., Quintero-Legorreta, O., García-Palomo, A., Macías, J.L., Alaniz-Álvarez, S.A., Nieto-Samaniego, A.F., Ferrari, L., 1999. Effect of strain rate in the distribution of monogenetic and polygenetic volcanism in the Transmexican volcanic belt: comments and reply. *Geology* 27 (6), 571–575 [http://dx.doi.org/10.1130/0091-7613\(1999\)027<0571:EORSRT>2.3.CO;2](http://dx.doi.org/10.1130/0091-7613(1999)027<0571:EORSRT>2.3.CO;2).
- Tauxe, L., Staudigel, H., 2004. Strength of the geomagnetic field in the Cretaceous Normal Superchron: new data from submarine basaltic glass of the Troodos Ophiolite. *Geochim. Geophys. Geosyst.* 5, Q02H06.
- Thellier, E., Thellier, O., 1959. Sur l'intensité du champ magnétique terrestre dans le passé historique et géologique. *Ann. Geophys.* 15, 285–378.
- Thorpe, R.S., 1977. Tectonic significance of alkaline volcanism in eastern Mexico. *Tectonophysics* 40 (3–4), T19–T26.
- Valentine, G.A., Connor, C.B., 2015. Basaltic volcanic fields. In: Sigurdsson, H., Houghton, B.F., McNutt, S.R., Rymer, H., Stix, J. (Eds.), *Encyclopedia of Volcanoes*, second ed. Academic Press, London, pp. 423–439.
- Yu, Y., Tauxe, L., 2005. Testing the IZZI protocol of geomagnetic field intensity determination. *Geochim. Geophys. Geosyst.* 6 (5):Q05H17. <http://dx.doi.org/10.1029/2004GC000840>.
- Yu, Y., Tauxe, L., Genevey, A., 2004. Toward an optimal geomagnetic field intensity determination technique. *Geochim. Geophys. Geosyst.* 5 (2):Q02H07. <http://dx.doi.org/10.1029/2003GC000630>.